Clinical Imaging 55 (2019) 156–160

Contents lists available at ScienceDirect

Clinical Imaging

journal homepage: www.elsevier.com/locate/clinimag

Body imaging

New radiologic classification of renal angiomyolipoma: frequently asked questions

Sung Goo Park, Byung Kwan Park*

Department of Radiology, Samsung Medical Center, Sungkyunkwan University School of Medicine, Seoul, Republic of Korea

ARTICLE INFO

Keywords:
Kidney
Angiomyolipoma
Carcinoma, renal cell
Multidetector computed tomography
Magnetic resonance imaging

ABSTRACT

Recently, a new classification of renal angiomyolipoma (AML) has been introduced to clinical practice. This classification categorizes AMLs into three subtypes (fat-rich, fat-poor, and fat-invisible AMLs) based on quantitative CT and MRI criteria. Radiologists who get used to previous AML classification may have questions about how to apply a new classification. The purpose of this review is to answer the questions that are frequently asked about the new AML classification.

1. Introduction

Angiomyolipoma (AML) is a very common benign renal tumor [1,2]. Most AMLs are not difficult to identify because the lesions have abundant fat, which can be easily detected using computed tomography (CT) or magnetic resonance imaging (MRI) [3–5]. In contrast, sometimes AMLs can be challenging to diagnose preoperatively if they have too little fat to be detected on CT or MRI [5–8]. Jinzaki et al. [6,7] first used the terminology "AML with minimal fat" to describe these unusual AML cases. However, investigators use various terminologies for these unusual AMLs, resulting in serious confusion to readers and other researchers [6,8–14].

Recently, two kinds of AML classification [3,4] were introduced in defining renal AMLs. One is the Jinzaki classification, published in 2014 [4], in which clinical, radiological, and pathological features are described for each AML subtype. The other classification was published in 2016 by Song et al. [3]. They reported a classification based only on radiological features, in which AML subtypes were classified according to quantitative CT or MRI features [3].

The Song classification significantly differs from the Jinzaki classification which might be confusing. The purpose of the current review is to answer questions that are frequently asked about these recent AML classifications.

2. Frequently asked questions

2.1. First question: do we really need a new classification of AML?

The Song classification is based only on radiological features. The subtypes of AML are determined by quantitative CT or MRI features (Table 1) [3,5,15]. Classifying AML subtypes is easy for a beginner, as well as an expert and demonstrates excellent inter-reader agreement between a resident and radiologist [3]. CT classifies fat-rich AML versus fat-poor AML, with a threshold of −10 HU (Figs. 1 and 2) [3,5]. MRI further differentiates fat-poor AML from fat-invisible AML, in which the tumor-to-spleen ratio (TSR) and signal intensity index (SII) are used on chemical shift imaging, with thresholds of 0.71 and 16.5%, respectively (Figs. 2 and 3) [3,5]. TSR is defined as (SI_{OP} of AML/SI_{OP} of spleen) / ($SI_{IP}$of AML/SI_{IP} of spleen) [3]. SII is defined as [(SI_{IP} ofAML − SI_{OP} of AML) × 100] / SI_{IP} of AML [3]. SI_{OP} and SI_{IP} indicated signal intensities on opposed-phase and in-phase images, respectively [3]. As a result, the Song classification is feasible and reproducible in classifying renal AMLs [3].

The Jinzaki classification does not provide quantitative MRI criteria (Table 1) [4]. Therefore, differentiating AML subtypes relies only on qualitative (visual) assessment to determine whether there is a signal drop on opposed-phase MRI. This subjective MRI criterion can influence

Abbreviations: AML, Angiomyolipoma; RCC, Renal cell carcinoma; CT, Computed tomography; MRI, Magnetic resonance imaging; ROI, Region of interest; TSR, Tumor to spleen ratio; SII, Signal intensity index

* Corresponding author at: Department of Radiology, Samsung Medical Center, Sungkyunkwan University School of Medicine, 81 Irwon-ro, Gangnam-ku, Seoul 06351, Republic of Korea.

E-mail address: rapark@skku.edu (B.K. Park).

https://doi.org/10.1016/j.clinimag.2019.01.025
Received 13 November 2018; Received in revised form 15 January 2019; Accepted 31 January 2019

Table 1
Comparison of AML subtypes in Song and Jinzaki classifications.

AML classification	AML subtypes	Imaging criteria	
		CT	MRI
Song classification	Fat-rich AML	−10 HU or less	NA
	Fat-poor AML	More than −10 HU	TSR < 0.71 or SII > 16.5%
	Fat-invisible AML	More than −10 HU	TSR ≥ 0.71 and SII ≤ 16.5%
Jinzaki classification	Classic AML	Less than −10 HU	NA
	Iso-attenuating AML	−10 HU–45 HU	[§]Positive CSI
	Hyperattenuating AML	> 45 HU	[§]Negative CSI

Note – AML, angiomyolipoma; NA, not applicable; TSR, tumor-to-spleen ratio; CSI, chemical shift imaging.
[§] Signal drop is visually assessed.

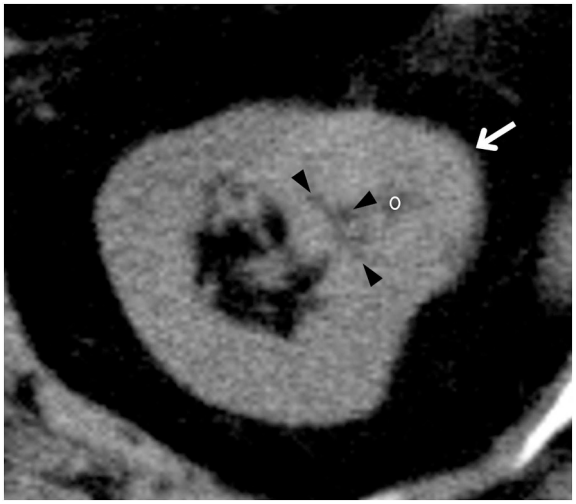

Fig. 1. Fat-rich AML in a 60-year-old woman.
An axial unenhanced CT image (3 mm section thickness) shows a left renal hyperdense mass (white arrow) containing multifocal hypodense areas. A region of interest (white circle) is placed in the most hypodense area, which is measured −62 HU. The other hypodense areas (black arrowheads) is also measured less than −10 HU. These finding are suggestive of a fat-rich AML.

the characterization of isoattenuating AML or hyperattenuating AML [3,5,15]. The Jinzaki classification classifies renal AML into two subgroups including sporadic AML and syndrome AML [4]. Sporadic AML consists of classical AML and fat-poor AML. Fat-poor AML includes isoattenuating AML, hyperattenuating AML, AML with epithelial cyst, and epitheliod AML. Syndrome AML consists of AML with tuberous sclerosis complex and AML with lymphangioleiomyomatosis. Therefore, AMLs with tuberous sclerosis complex is considered as another subtype [4]. However, this classification appears redundant in terms of differentiating sporadic and syndrome AMLs [4]. This is why AMLs with tuberous sclerosis can be described with the sporadic AML subtypes alone.

From this point of view, simplifying the AML classification with quantitative CT or MRI criteria helps standardize AML terminology, which will consequently enhance communication between researchers, and lead to appropriate management. Therefore, the Song classification may help radiologists to eliminate confusion resulting from the varied renal AML terminologies [5].

2.2. Second question: can renal AMLs be fully classified into three categories [16]?

Song et al. have shown that the subtypes of AML are not based on pathological features, but rather on radiological features alone (Table 1) [3,5]. If an AML measures −10 HU or less on CT, the subtype is defined as fat-rich AML (Fig. 1) [3,5]. If an AML measures more than −10 HU, the subtype should be fat-poor or fat-invisible AML [3,5]. If, on MRI, the TSR is < 0.71 or the SII is > 16.5%, then subtype is fat-poor AML (Fig. 2) [3,5], while fat-invisible AML is defined with a TSR of 0.71 or more and an SII of 16.5% or less (Fig. 3) [3,5]. Therefore, all AMLs can be classified into three categories as follows: fat-rich AML, fat-poor AML, and fat-invisible AML [15]. This question is usually posed by radiologists who are already familiar with the Jinzaki classification, in which classifying AMLs requires clinical, genetic, radiological, and histological considerations [16]. For example, patients with tuberous sclerosis complex tend to have multiple and bilateral AMLs [17], which can be fully categorized into the three subtypes of the Song classification. Tuberous sclerosis complex can be diagnosed with clinical background, radiological findings, and genetic analysis [18,19]. The main problems of these patients are sudden bleeding, abdominal distention, or progressive renal impairment due to rapid growth of AMLs [20–23]. After all, AML with tuberous sclerosis is not necessary in the Song classification because it is a radiologic classification.

The Jinzaki classification provides quantitative CT criteria, but not quantitative MRI criteria for AML classification (Table 1). Given these subjective MRI criteria, the results from different studies can vary, even though they are dealing with AMLs with a small amount of fat [10,24–26]. Moreover, these subjective MRI criteria have confused investigators, and thus varied terminology has been used to indicate AMLs with a small amount of fat [3,5,8].

2.3. Third question: can AML with epithelial cyst or epithelioid AML be classified using the Song classification [27]?

These AML subtypes do not exist in Song classification. These subtypes are extremely rare variants of AML [28–32]. Almost all have too little fat to be detected with CT or MRI [4,33]. Subsequently, they are classified as fat-invisible AML using the Song classification [4,34]. AML with epithelial cyst frequently manifests as a Bosniak III or IV cyst, so that these lesions are postoperatively diagnosed [4,28–30]. Epithelioid AML shows clinically malignant behavior, such as vein thrombosis, rupture, or metastasis [31,32,35,36]. These AML subtypes are almost impossible to preoperatively diagnose with CT or MRI. Furthermore, it is not easy to histologically confirm these AML subtypes using percutaneous biopsy alone [4]. Therefore, identifying these AML subtypes is beyond the ability of a radiologist [34]. Even though biopsy confirms epithelioid AML, the treatment plan cannot be altered because this subtype of AML should be surgically removed due to its malignant potential [35]. As a result, these variants can only be histologically classified, and cannot be categorized with radiological classification.

2.4. Fourth question: are fat-poor AML and fat-invisible AML on Song classification the same as isoattenuating AML and hyperattenuating AMLs on Jinzaki classification, respectively [27]?

Fat-poor AML on the Song classification is quite different from isoattenuating AML on the Jinzaki classification, in terms of diagnostic

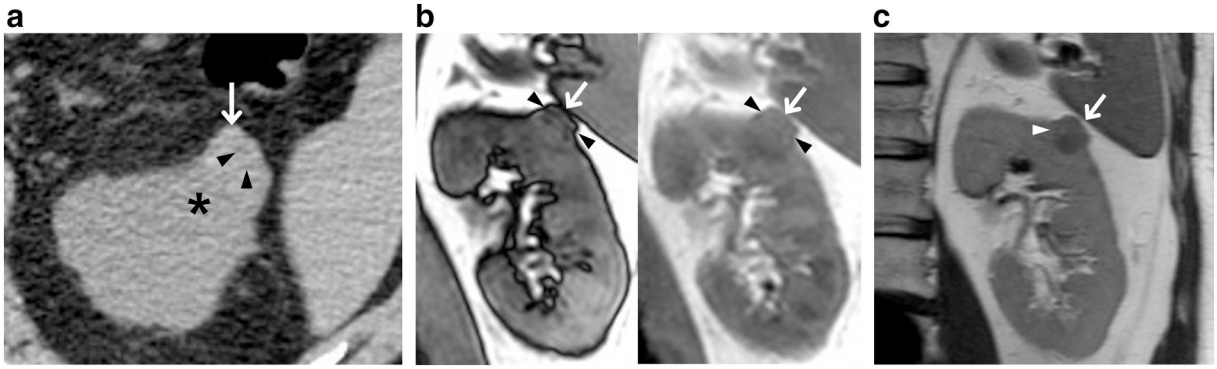

Fig. 2. Fat-poor AML in a 57-year-old man.
A. An axial unenhanced CT image shows a right renal hyperdense mass (white arrow) in which hypodense areas (black arrowheads) are measured 18–24 HU. The other area is more hyperdense than renal parenchyma (asterisk).
B. An opposed-phase coronal MR image (left side) shows focally hypointense areas (black arrowheads) in the right renal mass (white arrow). An in-phase axial MR image (right side) shows that the corresponding areas (black arrowhead) are isointense or slightly hyperintense. These findings suggest focal fat deposition. Tumor-to-spleen ratio and signal intensity index are 0.12 and 68.7%. This lesion was histologically confirmed as AML by percutaneous biopsy.
C. T2-weighted coronal MR image shows that the right renal mass (white arrow) is hypointense. A white arrowhead indicates a slightly hyperintense focus, which is well correlated with focal fat deposition on chemical shift MR image.

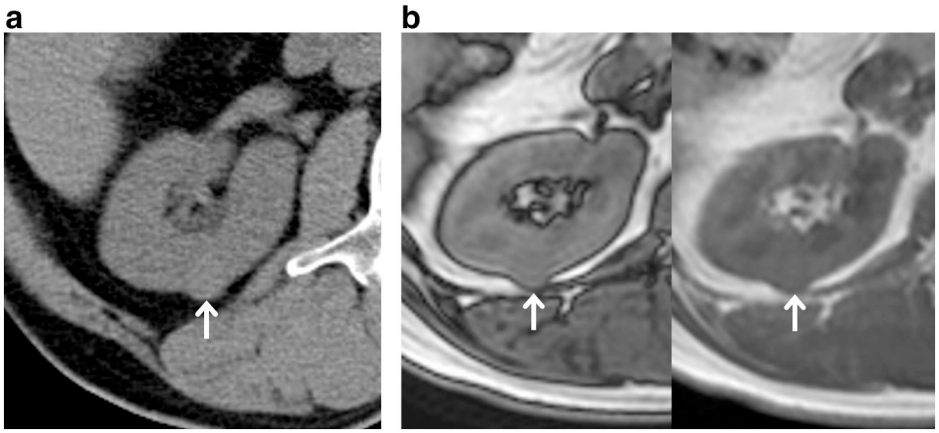

Fig. 3. Fat-invisible AML in a 54-year-old man.
A. An axial unenhanced CT image (3 mm section thickness) shows a right renal mass (white arrow) which is homogeneously hyperdense. The lesion attenuation value is measured 37 HU.
B. Opposed-phase (left side) and in-phase (right side) axial MR images show no signal change in the right renal mass (white arrow). Tumor-to-spleen ratio and signal intensity index are 1.32 and 1.2%. This lesion was histologically confirmed as AML by percutaneous biopsy.

criteria and imaging features (Table 1). On unenhanced CT, fat-poor AML is defined as a lesion that measures more than −10 HU [3], while isoattenuating AML is defined as a lesion that measures between −10 HU and 45 HU [4]. On chemical shift MRI, fat-poor AML is defined as a lesion in which the TSR is < 0.71 or the SII is > 16.5% (Fig. 2) [3], while isoattenuating AML does not have quantitative criteria [4]. Jinzaki et al. [4] defined isoattenuating AML as a lesion showing signal drop on opposed-phase MRI with visual assessment. Besides, this AML terminology is a misnomer because “isoattenuating” indicates that the renal mass density is the same as the renal parenchymal density. An isoattenuating AML which measures between −10 HU and 10 HU, appears as a hypoattenuating renal cyst [3,5]. Therefore, we wonder if this subtype can appropriately be named as an isoattenuating AML.

Fat-invisible AML on the Song classification appears to be similar to hyper-attenuating AML on the Jinzaki classification (Table 1). However, these AML subtypes totally differ from each other in terms of terminology definition. Fat-invisible AML is defined as a lesion with an attenuation value of more than −10 HU, a TSR of 0.71 or more, and a SII of 16.5% or less (Fig. 3). Hyper-attenuating AML is defined as a lesion in which attenuation value measures 45 HU or more and signal drop is absent on opposed phase MRI.

Another problem in the Jinzaki classification is that quantitative CT criteria is inconsistent with qualitative MRI assessment [3,5,15,34]. If an AML measures 20–45 HU, the lesion may not show signal drop on opposed phase MRI (Fig. 3). Although this AML cannot be categorized with the Jinzaki classification, the Song classification classes it as a fat-invisible AML. If an AML measures 45 HU or more, the lesion may show signal drop on opposed phase MRI. Again, although the Jinzaki classification cannot classify this AML, the Song classification can classify it as a fat-poor AML. Similar findings were also encountered when evaluating adrenal adenoma with CT and MRI [37–39].

The Song classification has also limitations. First, this classification does not provide any information on clinical findings, genetic background, histological findings, and prognosis because it is a radiologic classification. Second, this classification does not contain information on management based on genetic or histological findings, either. Therefore, this classification little suggests treatment plan or guideline.

2.5. *Fifth question: what subtypes of AML requires percutaneous biopsy?*

Generally, percutaneous biopsy is not recommended for fat-rich AML cases, because fat, which is a hallmark of AML, is easily identified on CT images (Table 2) [3–5]. Reportedly, however, fat can be detected in renal cell carcinomas (RCCs), although the incidence of this is extremely rare (Fig. 4). These unusual RCCs have characteristic imaging features. Large RCCs [40–44], relatively small fat foci [40–44], calcifications [42,45], cystic change [40], or necrosis [41,42] are frequently detected in fat-containing RCC (Fig. 4). Clinically, these RCCs are not so male dominant [40,44,45]. Percutaneous biopsy should be recommended to exclude a RCC when these radiological findings are detected in a renal mass with fat (Table 2).

The necessity of biopsy is still controversial in patients with fat-poor

Table 2
AML subtypes in Song classification: biopsy necessity and differential diagnosis.

Subtypes in Song classification	Necessity of biopsy	Differential diagnosis
Fat-rich AML	No but exceptionally Yes	Fat-containing RCC
Fat-poor AML	Still unknown	Clear cell RCC
Fat-invisible AML	Yes	Non-clear cell RCC

Note – AML, angiomyolipoma; RCC, renal cell carcinoma.

Fig. 4. Papillary RCC in a 50-year-old man.
An axial unenhanced CT image (3 mm section thickness) shows a left renal mass (white arrow), in which a hypodense area (white arrowhead) is measured −52 HU, suggesting fat. A black arrowhead indicates calcifications.

AML (Table 2) [3,5]. Many clear cell RCCs also show signal drops because of abundant intracytoplasmic lipid [25,46–48]. Thus, radiologists need to know how to differentiate fat-poor AML from clear-cell RCC. We have experienced characteristic patterns of signal drops in AML and RCC. Fat-poor AMLs tend to have a focal signal drop (Fig. 2) [3,5], while clear cell RCCs tend to have a diffuse signal drop (Fig. 5) [8]. Fat-poor AML in which signal drop is invisible, is hyperdense on unenhanced CT because of abundant muscle [3,5,8]. However, clear cell RCC is hypodense on unenhanced CT because of abundant intra-cytoplasmic lipid (Fig. 5) [3,5,8]. Moreover, T2-weighted MRI shows that fat-poor AMLs are hypointense as compared with renal parenchyma, whereas clear cell RCCs are hyperintense as compared with renal parenchyma (Figs. 2 and 5) [8]. Further investigation is necessary to validate these differential MRI features. Radiologists should not be reluctant to perform biopsy if discriminating AMLs and RCCs are not clear on chemical shift MRI.

Fat-invisible AML should be biopsied to exclude non-clear cell RCC for the same reason than hyperattenuating AML (Table 2) [8,49]. Both lesions appear homogeneously hyper-attenuating on unenhanced CT, hypointense on T2-weighted MRI, and homogeneously enhancing on contrast-enhanced CT and MRI [49–51]. For this reason, we cannot rely on CT or MRI features to differentiate fat-invisible AMLs and non-clear cell RCCs. Biopsy is essential for patients with fat-invisible AML to avoid unnecessary surgery.

2.6. Sixth question: how should a region of interest (ROI) be drawn for fat detection?

The size or location of a ROI is of great importance to classify renal AMLs [3,5]. The following steps are necessary for precise fat detection. First, great care should be taken to find a hypo-attenuating area on CT images or a hypo-intense area on opposed MR images [3,5]. Second, the size or shape of a ROI should be controlled to fit within the margin of fat (Fig. 1) [3,5]. A ROI should not be drawn beyond the margin of fat to avoid partial volume effect. Slice thickness should necessarily be < 5 mm [4]. Fat may be missed if the slice thickness is 5 mm or more. Third, the corresponding area should be searched on in-phase MR images [3,5]. Currently-available MRI scanners provide dual-echo sequencing to simultaneously obtain both in-phase and opposed phase images [8,39]. Thus, it is not difficult to detect the corresponding area on in-phase MRI to calculate the TSR or SII. Ideally, as it is allowed by some software, the ROI could be copy-pasted from one image to another, copying exact location and size. For a fat-rich or fat-poor AML, the size or location of a ROI is crucial for characterization and classification. For a fat-invisible AML, the size or location of a ROI is not a major problem because the lesion texture is homogeneous.

Song et al. [3] demonstrated that only a small number of AMLs analysis and classification were discordant between a resident and a radiologist. Most of discordances resulted from the inappropriate size or location of the ROI [3]. Therefore, controlling the ROI is the most important step for precise fat detection.

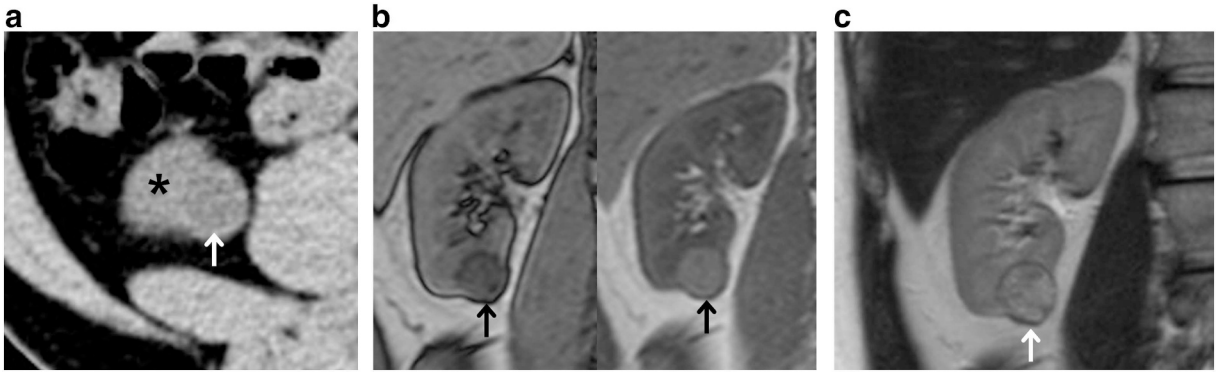

Fig. 5. Clear cell RCC in a 66-year-old man.
A. An axial unenhanced CT image shows a right renal mass (white arrow) which is more hypodense than renal parenchyma (asterisk). The lesion attenuation value is 21 HU.
B. An opposed-phase axial MR image (left side) shows a diffusely hypointense area in the right renal mass (black arrow). An in-phase axial MR image (right side) shows that the lesion (black arrow) is diffusely hyperintense. Tumor-to-spleen ratio and signal intensity index are 0.34 and 42.6%, respectively.
C. T2-weighted coronal MR image shows the lesion (white arrow) is heterogeneously hyperintense. These findings suggest abundant intracytoplasmic lipid. This lesion was histologically confirmed as a clear cell RCC by surgery.

3. Conclusion

Two kinds of AML classifications are now available for clinical practice. Since the Song classification is based on objective CT and MRI criteria, it can help enhancing terminology standardization and improving inter-researcher communication. Being familiar with the answers to these frequently asked questions could help understanding of the new radiological classification of renal AMLs.

Acknowledgment

This study has been conducted without any fund.
None of authors have conflict of interest.
IRB approval or patient consent was not applicable because this paper is a review article.

References

[1] Fujii Y, Komai Y, Saito K, Iimura Y, Yonese J, Kawakami S, et al. Incidence of benign pathologic lesions at partial nephrectomy for presumed RCC renal masses: Japanese dual-center experience with 176 consecutive patients. Urology 2008;72:598–602.
[2] Jeon HG, Lee SR, Kim KH, Oh YT, Cho NH, Rha KH, et al. Benign lesions after partial nephrectomy for presumed renal cell carcinoma in masses 4 cm or less: prevalence and predictors in Korean patients. Urology 2010;76:574–9.
[3] Song S, Park BK, Park JJ. New radiologic classification of renal angiomyolipomas. Eur J Radiol 2016;85:1835–42.
[4] Jinzaki M, Silverman SG, Akita H, Nagashima Y, Mikami S, Oya M. Renal angiomyolipoma: a radiological classification and update on recent developments in diagnosis and management. Abdom Imaging 2014;39:588–604.
[5] Park BK. Renal angiomyolipoma: radiologic classification and imaging features according to the amount of fat. AJR Am J Roentgenol 2017;209:826–35.
[6] Jinzaki M, Tanimoto A, Narimatsu Y, Ohkuma K, Kurata T, Shinmoto H, et al. Angiomyolipoma: imaging findings in lesions with minimal fat. Radiology 1997;205:497–502.
[7] Jinzaki M, Silverman SG, Tanimoto A, Shinmoto H, Kuribayashi S. Angiomyolipomas that do not contain fat attenuation at unenhanced CT. Radiology 2005;234:311. (author reply -2).
[8] Jeong CJ, Park BK, Park JJ, Kim CK. Unenhanced CT and MRI parameters that can be used to reliably predict fat-invisible angiomyolipoma. AJR Am J Roentgenol 2016;206:340–7.
[9] Chaudhry HS, Davenport MS, Nieman CM, Ho LM, Neville AM. Histogram analysis of small solid renal masses: differentiating minimal fat angiomyolipoma from renal cell carcinoma. AJR Am J Roentgenol 2012;198:377–83.
[10] Dillon RC, Friedman AC, Miller FH. MR signal intensity calculations are not reliable for differentiating renal cell carcinoma from lipid poor angiomyolipoma. Radiology 2010;257:299–300. (author reply).
[11] Milner J, McNeil B, Alioto J, Proud K, Rubinas T, Picken M, et al. Fat poor renal angiomyolipoma: patient, computerized tomography and histological findings. J Urol 2006;176:905–9.
[12] Kim JY, Kim JK, Kim N, Cho KS. CT histogram analysis: differentiation of angiomyolipoma without visible fat from renal cell carcinoma at CT imaging. Radiology 2008;246:472–9.
[13] Choi HJ, Kim JK, Ahn H, Kim CS, Kim MH, Cho KS. Value of T2-weighted MR imaging in differentiating low-fat renal angiomyolipomas from other renal tumors. Acta Radiol 2011;52:349–53.
[14] Simpfendorfer C, Herts BR, Motta-Ramirez GA, Lockwood DS, Zhou M, Leiber M, et al. Angiomyolipoma with minimal fat on MDCT: can counts of negative-attenuation pixels aid diagnosis? AJR Am J Roentgenol 2009;192:438–43.
[15] Park BK. Reply: can angiomyolipomas be classified fully into three types? Eur J Radiol 2017;96:117–8.
[16] Jinzaki M, Silverman SG. Can angiomyolipomas be classified fully into three types? Eur J Radiol 2017;96:115–6.
[17] Manoukian SB, Kowal DJ. Comprehensive imaging manifestations of tuberous sclerosis. AJR Am J Roentgenol 2015;204:933–43.
[18] Northrup H, Krueger DA. Tuberous sclerosis complex diagnostic criteria update: recommendations of the 2012 International Tuberous Sclerosis Complex Consensus Conference. Pediatr Neurol 2013;49:243–54.
[19] Teng JM, Cowen EW, Wataya-Kaneda M, Gosnell ES, Witman PM, Hebert AA, et al. Dermatologic and dental aspects of the 2012 international tuberous sclerosis complex consensus statements. JAMA Dermatol 2014;150:1095–101.
[20] Simmons JL, Hussain SA, Riley P, Wallace DM. Management of renal angiomyolipoma in patients with tuberous sclerosis complex. Oncol Rep 2003;10:237–41.
[21] Harabayashi T, Shinohara N, Katano H, Nonomura K, Shimizu T, Koyanagi T. Management of renal angiomyolipomas associated with tuberous sclerosis complex. J Urol 2004;171:102–5.
[22] Hadley DA, Bryant LJ, Ruckle HC. Conservative treatment of renal angiomyolipomas in patients with tuberous sclerosis. Clin Nephrol 2006;65:22–7.
[23] Brakemeier S, Bachmann F, Budde K. Treatment of renal angiomyolipoma in tuberous sclerosis complex (TSC) patients. Pediatr Nephrol 2017;32:1137–44.
[24] Kim JK, Kim SH, Jang YJ, Ahn H, Kim CS, Park H, et al. Renal angiomyolipoma with minimal fat: differentiation from other neoplasms at double-echo chemical shift FLASH MR imaging. Radiology 2006;239:174–80.
[25] Hindman N, Ngo L, Genega EM, Melamed J, Wei J, Braza JM, et al. Angiomyolipoma with minimal fat: can it be differentiated from clear cell renal cell carcinoma by using standard MR techniques? Radiology 2012;265:468–77.
[26] Sasiwimonphan K, Takahashi N, Leibovich BC, Carter RE, Atwell TD, Kawashima A. Small (< 4 cm) renal mass: differentiation of angiomyolipoma without visible fat from renal cell carcinoma utilizing MR imaging. Radiology 2012;263:160–8.
[27] Sureka B, Khera PS. Radiologic classification and imaging features of renal angiomyolipomas according to the amount of fat. AJR 2018;210:XXX-XXX.
[28] Fine SW, Reuter VE, Epstein JI, Argani P. Angiomyolipoma with epithelial cysts (AMLEC): a distinct cystic variant of angiomyolipoma. Am J Surg Pathol 2006;30:593–9.
[29] Armah HB, Yin M, Rao UN, Parwani AV. Angiomyolipoma with epithelial cysts (AMLEC): a rare but distinct variant of angiomyolipoma. Diagn Pathol 2007;2:11.
[30] Acar T, Harman M, Sen S, Kumbaraci BS, Elmas N. Angiomyolipoma with epithelial cyst (AMLEC): a rare variant of fat poor angiomyolipoma mimicking malignant cystic mass on MR imaging. Diagn Interv Imaging 2015;96:1195–8.
[31] Vicens RA, Jensen CT, Korivi BR, Bhosale PR. Malignant renal epithelioid angiomyolipoma with liver metastasis after resection: a case report with multimodality imaging and review of the literature. J Comput Assist Tomogr 2014;38:574–7.
[32] Cho SW, Choi HJ, Lee S. Rapidly progressing malignant epithelioid renal angiomyolipoma: a case report. Urol J 2016;13:2653–5.
[33] Tsukada J, Jinzaki M, Yao M, Nagashima Y, Mikami S, Yashiro H, et al. Epithelioid angiomyolipoma of the kidney: radiological imaging. Int J Urol 2013;20:1105–11.
[34] Park BK. Reply to Radiologic classification and imaging features of renal angiomyolipomas according to the amount of fat. AJR 2018;210. (XXX-XXX).
[35] Delhorme JB, Fontana A, Levy A, Terrier P, Fiore M, Tzanis D, et al. Renal angiomyolipomas: at least two diseases. A series of patients treated at two European institutions. Eur J Surg Oncol 2017;43:831–6.
[36] Yoshida Y, Minato N, Takada T, Koga M, Sugao H, Nakamichi I. Renal epithelioid angiomyolipoma with spontaneous rupture: a case report. Hinyokika Kiyo 2015;61:437–40.
[37] Haider MA, Ghai S, Jhaveri K, Lockwood G. Chemical shift MR imaging of hyperattenuating (> 10 HU) adrenal masses: does it still have a role? Radiology 2004;231:711–6.
[38] Park BK, Kim CK, Kim B, Lee JH. Comparison of delayed enhanced CT and chemical shift MR for evaluating hyperattenuating incidental adrenal masses. Radiology 2007;243:760–5.
[39] Seo JM, Park BK, Park SY, Kim CK. Characterization of lipid-poor adrenal adenoma: chemical-shift MRI and washout CT. AJR Am J Roentgenol 2014;202:1043–50.
[40] Richmond L, Atri M, Sherman C, Sharir S. Renal cell carcinoma containing macroscopic fat on CT mimics an angiomyolipoma due to bone metaplasia without macroscopic calcification. Br J Radiol 2010;83:e179–81.
[41] Lesavre A, Correas JM, Merran S, Grenier N, Vieillefond A, Helenon O. CT of papillary renal cell carcinomas with cholesterol necrosis mimicking angiomyolipomas. AJR Am J Roentgenol 2003;181:143–5.
[42] Helenon O, Merran S, Paraf F, Melki P, Correas JM, Chretien Y, et al. Unusual fat-containing tumors of the kidney: a diagnostic dilemma. Radiographics 1997;17:129–44.
[43] D'Angelo PC, Gash JR, Horn AW, Klein FA. Fat in renal cell carcinoma that lacks associated calcifications. AJR Am J Roentgenol 2002;178:931–2.
[44] Hammadeh MY, Thomas K, Philp T, Singh M. Renal cell carcinoma containing fat mimicking angiomyolipoma: demonstration with CT scan and histopathology. Eur Radiol 1998;8:228–9.
[45] Helenon O, Chretien Y, Paraf F, Melki P, Denys A, Moreau JF. Renal cell carcinoma containing fat: demonstration with CT. Radiology 1993;188:429–30.
[46] Jhaveri KS, Elmi A, Hosseini-Nik H, Hedgire S, Evans A, Jewett M, et al. Predictive value of chemical-shift MRI in distinguishing clear cell renal cell carcinoma from non-clear cell renal cell carcinoma and minimal-fat angiomyolipoma. AJR Am J Roentgenol 2015;205:W79–86.
[47] Outwater EK, Bhatia M, Siegelman ES, Burke MA, Mitchell DG. Lipid in renal clear cell carcinoma: detection on opposed-phase gradient-echo MR images. Radiology 1997;205:103–7.
[48] Yoshimitsu K, Honda H, Kuroiwa T, Irie H, Tajima T, Jimi M, et al. MR detection of cytoplasmic fat in clear cell renal cell carcinoma utilizing chemical shift gradient-echo imaging. J Magn Reson Imaging 1999;9:579–85.
[49] Silverman SG, Israel GM, Herts BR, Richie JP. Management of the incidental renal mass. Radiology 2008;249:16–31.
[50] Israel GM, Silverman SG. The incidental renal mass. Radiol Clin North Am 2011;49:369–83.
[51] Sahni VA, Silverman SG. Imaging management of incidentally detected small renal masses. Semin Intervent Radiol 2014;31:9–19.